Brain, Behavior, & Immunity - Health 30 (2023) 100616

Contents lists available at ScienceDirect

Brain, Behavior, & Immunity - Health

journal homepage: www.editorialmanager.com/bbih/default.aspx

Full Length Article

Inflammatory hallmarks in 6-OHDA- and LPS-induced Parkinson's disease in rats

Zhanna Oliynyk [a], Mariia Rudyk [a,*], Taisa Dovbynchuk [a], Nataliia Dzubenko [a], Ganna Tolstanova [b], Larysa Skivka [a]

[a] Educational and Scientific Centre "Institute of Biology and Medicine", Taras Shevchenko National University of Kyiv, 2, Hlushkov Avenue, Kyiv, 03022, Ukraine
[b] Educational and Scientific Institute of High Technologies, Taras Shevchenko University of Kyiv, 4g, Hlushkova Avenue, Kyiv, 03022, Ukraine

ARTICLE INFO

Keywords:
6-Hydroxydopamine
Lipopolysaccharide
Microglia/macrophages
Parkinson's disease
Neuroinflammation
Systemic inflammation

ABSTRACT

Parkinson's disease (PD) is the second most common neurodegenerative disease, affecting more than 1% of aged people. PD, which was previously identified as movement disorder, now is recognized as a multi-factorial systemic disease with important pathogenetic and pathophysiological role of inflammation. Reproducing local and systemic inflammation, which is inherent in PD, in animal models is essential for maximizing the translation of their potential to the clinic, as well as for developing putative anti-inflammatory neuroprotective agents. This study was aimed to compare activation patterns of microglia/macrophage population and systemic inflammation indices in rats with 6-Hydroxydopamine (6-OHDA)- and Lipopolysaccharide (LPS)-induced PD. Metabolic and phenotypic characteristics of microglia/macrophage population were examined by flow cytometry, systemic inflammatory markers were calculated using hematological parameters in 6-OHDA- and LPS-lesioned Wistar rats 29 days after the surgery.

Microglia/macrophages from rats in both models exhibited pro-inflammatory metabolic shift. Nevertheless, in LPS-lesioned animals, highly increased proportion of CD80/86+ cells in microglia/macrophage population was registered alongside increased values of systemic inflammatory indices: neutrophil to lymphocyte ratio (NLR), derived neutrophil to lymphocyte ratio (dNLR), platelet to lymphocyte ratio and systemic immune inflammation index (SII). There was significant positive correlation between the count of CD80/86+ cells and systemic inflammatory indices in these animals. Microglia/macrophages from 6-OHDA-lesioned rats were characterized by the increased fraction of CD206+ cells alongside decreased proportion of CD80/86+ cells. No signs of systemic inflammation were observed. Negative correlation between quantitation characteristics of CD80/86+ cells and values of systemic inflammatory indices was registered. Collectively, our data show that LPS-PD model unlike 6-OHDA-PD replicates crosstalk between local and systemic inflammatory responses, which is inherent in PD pathogenesis and pathophysiology.

1. Introduction

Parkinson's disease (PD) is the second most common age-related neurodegenerative disorder. PD morbidity is predicted to rise progressively considering a rapid ageing of the population worldwide. More than 90% of PD cases have unknown causes and are idiopathic in nature (Tysnes and Storstein, 2017). The exact mechanisms underlying PD pathogenesis are yet to be established. However, PD, which was previously identified as movement disorder, now is recognized as a multi-factorial systemic disease, and important role in disease pathogenesis is given to immune system (Öberg et al., 2021; Tansey et al., 2022). Moreover, recent studies in the PD immunogenetics allowed to reveal some immune-related genes involved in the pathogenesis of both familial and idiopathic disease forms (Chen et al., 2022; Magistrelli et al., 2022). Chronic microglia-mediated neuroinflammation is one of the hallmarks of PD pathophysiology (Wang et al., 2015; Muzio et al., 2021). Lately, microgliosis has been considered as one of the probable pathogenetic mechanisms of PD (Troncoso-Escudero et al., 2018; MacMahon Copas et al., 2021; Zhu et al., 2022). Microglia are the most abundant resident immunocytes in the central nervous system (CNS), where they closely interact with astrocytes and

* Corresponding author. Microbiology and Immunology Department, ESC "Institute of Biology and Medicine", Taras Shevchenko Kyiv National University, Kyiv, 2, Hlushkov Avenue, Kyiv, 03022, Ukraine.
E-mail address: rosiente@gmail.com (M. Rudyk).

https://doi.org/10.1016/j.bbih.2023.100616
Received 6 January 2023; Received in revised form 17 March 2023; Accepted 27 March 2023
Available online 5 April 2023

Abbreviations

ALC	Absolute lymphocyte count
AMC	Absolute monocyte count
ANC	Absolute neutrophil count
APC	Absolute platelet count
BBB	The blood-brain barrier
CNS	The central nervous system
DN	Dopaminergic neurons
dNLR	Derived neutrophil to lymphocyte ratio
FITC	Fluorescein isothiocyanate
LMR	Lymphocyte to monocyte ratio
LPS-PD	Lipopolysaccharide-induced PD
MC	The modulation coefficient
NLR	Neutrophil to lymphocyte ratio
PD	Parkinson's disease
PE	Phycoerythrin
PhI	Phagocytosis index
PLR	platelet to lymphocyte ratio
PMA	Phorbol 12-myristate 13-acetate
PP	Phagocytosis percentage
ROS	Reactive oxygen species
SII	Systemic immune inflammation index
SIRI	Systemic inflammatory response index
TH	Tyrosine hydroxylase
WBC	White blood cell count

neurons both physically and functionally, participating in tissue homeostasis and immune defense (Ho, 2019; Zhao et al., 2021). Resident microglial cells originate from the yolk sac and differ from resident macrophages in peripheral tissues in their unique phenotypic and metabolic features. Microglial cells have the ability of self-renewal and repopulation, and in such a way they maintain constant cell density in healthy adult brain (Lee E. et al., 2021; Zeng et al., 2022). In physiological conditions, these resident sentinel cells are supposed to be a slightly shifted toward an anti-inflammatory (M2) phenotype, which is valuable to brain homeostasis (Cherry et al., 2014; Jurga et al., 2020). In pathological conditions, such as neurodegeneration, polarized activation of the microglia (pro-inflammatory shifted vs anti-inflammatory) can mediate neuroinflammation or its resolution exacerbating or relieving disease progression correspondingly (Abellanas et al., 2019; Lashgari et al., 2021; Lee J.W. et al., 2021). It should also be noted that microglia pro-inflammatory activation in these circumstances can be both the trigger of neuron loss and the consequence of the neurodegeneration. On the one hand, numerous external stimuli including peripheral inflammatory mediators associated with systemic inflammation, gut dysbiosis etc. can trigger pro-inflammatory microglia activation preceding neurodegeneration (Agirman et al., 2021). On the other hand, neuron degeneration, which is accompanied by the release of Damage-Associated Molecular Patterns (High Mobility Group Box 1 proteins (HMGB1), mitochondrial transcription factor A (TFAM), cardiolipin, succinate, N-formyl peptides, mitochondrial DNA etc.), can urge pro-inflammatory microglia shift (Gelders et al., 2018). Neuroinflammation is always associated with the impairment of the blood-brain barrier (BBB). Activated microglia produce matrix metalloproteinases, reactive oxygen and nitrogen species, chemokines, inflammatory cytokines such as tumor necrosis factor (TNF-α), interleukin-1β (IL-1β), IL-2, IL-6 etc., and can phagocytize astrocytic end-feet. These can cause impairment of the BBB function through the downregulation of tight junction molecules and disturbance of the trans-endothelial electrical resistance, as well as permeability parameters (Haruwaka et al., 2019; Huang et al., 2021; Hourfar et al., 2023). Microglia activation and BBB disruption followed by the recruitment of circulating monocytes into the CNS where these cells differentiate into blood-born derived macrophages (Takata et al., 2021; Gaviglio et al., 2022). These blood-borne phagocytes in the complex microglia/macrophage population represent an additional crucial cellular component in mediating neuroinflammation. Metabolic profile of the complex population of phagocytes determines the course of chronic inflammatory disease of the CNS such as neurodegenerative disorders and is considered as an attractive therapeutic target for the treatment of these pathologies (Sevenich, 2018; Grassivaro et al., 2021; Miao et al., 2022).

Growing body of evidence suggests involving systemic inflammation (SI) in PD pathophysiology and pathogenesis. In addition, the crosstalk between the local neuroinflammation and SI, between the central and peripheral immune systems in PD has attracted attention in recent decade (Tansey et al., 2022; Zhu et al., 2022). Aforementioned peripheral low-level chronic inflammation may stimulate neuroinflammation in the conditions of the increased BBB permeability, and thereby promote PD initiation and/or aggravation (Dogra et al., 2022; Zeng et al., 2022). Neuroinflammation, in turn, may initiate, maintain and exacerbate SI. Chronically activated microglia release high levels of pro-inflammatory mediators which can be exported to the periphery initiating/provoking systemic immune responses, and in such a way creating self-sustained inflammatory vicious circle. Both central and systemic inflammation targeting may hold a promise in slowing-down or stop neurodegeneration in PD (Araújo et al., 2022; Gundersen, 2021).

Reproducing this integrated network of central and peripheral inflammation in animal models is required for advancing the understanding of the disease pathogenesis and is relevant to definition of possible therapeutic targets (Lama et al., 2021). Among different rodent PD models, immune-related model induced by intracerebral injection of bacterial lipopolysaccharide (LPS-PD) along with classic toxic model induced by 6-hydroxydopamine (6-OHDA-PD) are most widely used, since these models most faithfully recapitulate many aspects of PD clinical picture including motor impairment and non-motor symptoms. Although LPS is a direct pro-inflammogen, whereas 6-OHDA belongs to the toxins causing the specific death of dopaminergic neurons, neuroinflammation in these two models also exhibits many common features and occurs as a common mechanism to different molecular triggers. Pro-inflammatory microglia activation in both these interventional models is TLR4-dependent, is associated with BBB impairment and brain infiltration with peripheral myeloid and lymphoid immune cells, and is accompanied by the release of neurotoxic inflammatory mediators by these immunocytes (García-Revilla et al., 2022). Nevertheless, although neuroinflammatory responses induced by LPS and 6-OHDA share many common features, their mechanisms vary considering involvement of different receptors and signaling pathways (Rosadini and Kagan, 2017; Gopinath et al., 2022). SI manifestation in these two models is virtually unexplored. We have shown previously that signs of systemic inflammation manifest in different ways in rats with LPS-PD and 6-OHDA-PD. In LPS-PD, decreased circulating lymphocyte fraction along with increased neutrophil count as well as pro-inflammatory functional shift of circulating monocytes and granulocytes were registered (Oliynyk et al., 2022). In 6-OHDA-PD, increased monocyte fraction along with anti-inflammatory polarization of these cells and circulating granulocytic neutrophils were observed. We hypothesized that these differences in systemic inflammation manifestation would be associated with distinctions in microglia activation patterns. To address this, our study was aimed to compare activation patterns of microglia/macrophage population and systemic inflammation indices in rats with 6-OHDA- and LPS-induced PD.

2. Materials and methods

2.1. Animals and study design

Experiments were conducted on adult male Wistar rats (220–250 g) bred in the vivarium of the Educational and Scientific Centre "Institute of Biology and Medicine" of Taras Shevchenko National University of Kyiv, Ukraine. The animals were kept in standard conditions with ad libitum access to water and food (standard diet). Animal protocols were approved by the University Ethics Committee (protocol No 4, October 10, 2021) according to Animal Welfare Act guidelines. All procedures with animals were performed in accordance with the principles of humanity as it was written in "General principles of animal experimentation" approved by the National Congress on bioethics (Kyiv, 2001–2007) and in concordance with Council directive of November 24, 1986 on the approximation of laws, regulations and administrative provisions of the Member States regarding the protection of animals used for experimental and other scientific purposes (86/609/EEC). PD development was ascertained by the results of behavioral testing and post-mortem assessment of nigrostriatal neurodegeneration using semi-quantitative tyrosine hydroxylase (TH) immunohistochemistry. Hematological indices and metabolic profile of microglia/macrophage population were evaluated at the time point of the experiment cessation (day 29 after the surgery). The time point of the experiment cessation was determined in keeping to time-course of nigrostriatal damage in 6-OHDA-PD model. According to the literature data, DA lesions in this model exhibit fast changes from week 2 to week 3 post-injection, peaked at the 28th day, and maintained kept a stable state with the tendency to spontaneous recovery from week 3 to week 6 (Blandini et al., 2007; Su et al., 2018).

2.2. 6-OHDA-PD model

Before the experiment, 30 adult male Wistar rats were randomly selected and arranged into 3 groups: group I - intact animals (n = 10); group II - sham-operated animals (n = 10); group III - 6-OHDA-PD (n = 10). In order to attain unilateral lesions of the nigrostriatal system in animals from group III, stereotaxic microinjections of 12 μg of selective neurotoxin 6-OHDA (Sigma, USA) in the medial forebrain bundle (MFB) were conducted (Talanov et al., 2006). For the injection, 6-OHDA was solved in 4.0 μL of sterile physiological saline (JSC "Infusion", Ukraine) supplemented with 0.1% ascorbic acid for preventing 6-OHDA oxidation. Animals from group II (sham-operated) were injected with 4.0 μL of sterile physiological saline. Before the surgery, animals from groups II and III were anesthetized with nembutal (50 mg/kg, i.p., "Sigma", USA), placed in a stereotaxic instrument (SEJ-4, Ukraine), and were then injected i.p. with 40 mg/kg pargyline (Sigma, USA), which inhibits the metabolic conversion of 6-OHDA by monoamine oxidase, and 25 mg/kg desipramine (Sigma, USA), which blocks the uptake of neurotoxin by noradrenergic neurons. In 30 min, animals were scalped and trepanned by using following coordinates (mm) from the bregma (AP = −2.2; ML = 1.5; DV = 8.8) (Paxinos and Watson, 2007). After that, either 6-OHDA or sterile physiological saline were injected into the brain through the drilled burr hole at 8.8 mm depth. The injections were performed at a rate of 1 μl/min (every 15s). The injector was left in place for 5 min before being slowly withdrawn to allow for toxin diffusion and prevent the toxin reflux.

2.3. LPS-PD model

Before the experiment, 30 adult male Wistar rats were randomly selected and arranged into 3 groups: group I - intact animals (n = 10); group II - sham-operated animals (n = 10); group III - LPS-PD (n = 10). In order to attain unilateral lesions of the nigrostriatal system in animals from group III, stereotaxic microinjections of 10 μg of LPS (Lipopolysaccharides from *Escherichia coli* O111:B4, Sigma) at the volume of 2 μl of sterile physiological saline (JSC "Infusion", Ukraine) were conducted. Animals from group II (sham-operated) were injected with 2.0 μL of sterile physiological saline. Before the surgery, rats from groups II and III were anesthetized with a mixture of ketamine (75 mg/kg diluted in sterile water for injection, Sigma, USA) and 2% Xylazine (400 μl/kg, Alfasan International BV, Netherlands) i.p, placed in a stereotaxic instrument (SEJ-4, Ukraine). After that, either LPS or sterile physiological saline were injected into the brain through the drilled burr hole directly into the substantia nigra (AP = −5.3; ML = ± 2.0; DV = −7.2) according to Hoban et al. (2013) at 8.8 mm depth. All microinjections were performed as described in 2.2.

2.4. Behavioral testing

Open field test was conducted 28 days after the surgery as described earlier (Leite-Almeida et al., 2009). To evaluate voluntary movement, anxiety, and exploratory behavior in the new environment, the rats were tested in the Open Field arena (a square field with sides of 100 cm and a wall height of 30 cm, which illuminated by two LED lamps (each with 60W) placed at a height of 2 m) for 5 min. A grid of 36 squares was drawn on the bottom of the arena. During testing, each animal was individually placed in the center of the arena and its ambulatory activity was recorded using a digital camera ("Casio® EX-Z850", China, which was located above the center of the arena at a height of 1 m) followed by the analysis using MATLAB. The following behavioral characteristics were assessed: locomotor activity (total distance traveled in the session represented as total number of crossed squares, number of rearing and grooming (vertical activity) in the session); anxiety-like behavior (decreased total locomotor activity, decreased entries to the inner zone, increased latency to start movement, increased frequency of defecations) (Sestakova et al., 2013). After each animal was tested, the arena was cleansed and allowed to dry.

Apomorphine test was conducted 7 and 14 days after the surgery. Apomorphine (Sigma, USA) was i.p. administered to the lesioned rats at a dose of 0.5 mg/kg. Five minutes after the injection, the rats were individually put into a 40 cm-diameter cylinder and the counterclockwise (contralateral) rotations were monitored and registered for 30 min using a stopwatch (Smith et al., 2012). Animals scoring over 6 rpm were considered as lesioned with 86.6% DN loss. Rats scoring less than 6 rpm (0–2 rpm) were considered as lesioned with 44% DN loss (Talanov et al., 2006).

2.5. Immunohistochemistry

For immunohistochemical staining of rat brain sections with antibodies to tyrosine hydroxylase (TH), rats were deeply anesthetized and transcardially perfused with heparinised (5000 U/L) sterile physiological saline (100 ml) followed by 4% paraformaldehyde (150 mL, pH 7.4). The brains were removed, post-fixed in 4% paraformaldehyde and then sectioned. The paraffin-embedded sections (5 μm) were processed for TH immunohistochemical detection using ABC–peroxidase method as described previously (Walsh et al., 2011). Briefly, tissue sections were first incubated with tyrosine hydroxylase (TH) primary antibodies (1:200, Millipore, AB152, USA) overnight (4 °C), and then with the secondary anti-rabbit biotinylated antibodies (1:200) for 60 min. After this, Diaminobenzidine (Dako, EnVision Flex, DM821, USA) immunoreactivity detection system was applied for 5 min. Stained sections were assessed using a Primo Star microscope, Zeizz. Each sample was scored semi-quantitatively as to the intensity of immunostaining on a four-point scale, with 0 indicating absence of staining (<10% of positive cells), 1+ indicating the lowest level of detectable staining (10–25% of positive cells), 2+ indicating moderate homogeneous staining (25–50% of positive cells), 3+ indicating intense homogeneous staining (50–75% of positive cells), and 4+ (>75% of positive cells) (Pauletti et al., 2000). Results are then scored by multiplying the percentage of positive cells (P) by the intensity (I) and presented as Quick score (Q): Q = P x I.

2.6. Hemogram analysis

Hematological indices were examined using an analyzer "Particle counter model PCE 210" (ERMA, Japan), adapted to the study of blood cells in rats and mice. Neutrophil to lymphocyte ratio (NLR), derived neutrophil to lymphocyte ratio (dNLR), lymphocyte to monocyte ratio (LMR), platelet to lymphocyte ratio (PLR), systemic inflammatory response index (SIRI), and systemic immune inflammation index (SII) were determined. NLR = absolute neutrophil count (ANC)/absolute lymphocyte count (ALC); dNLR = ANC/(white blood cell count (WBC) − ANC); LMR = (ALC)/absolute monocyte count (AMC); PLR = absolute platelet count (APC)/ALC; SII = (ANC × APC)/ALC; SIRI = (ANC × AMC)/ALC) (Hu et al., 2014).

2.7. Microglia/macrophage cell isolation

For microglia/macrophage cells isolation, brain was rapidly extracted on ice. Hippocampus was dissected and perfused using a phosphate buffered saline (PBS). Isolated tissue was softly dissociated in ice cold PBS supplemented with 0.2% glucose for 15 min at room temperature using Potter homogenizer. Tissue homogenate was filtered through a 40 nm cell strainer (BD Biosciences Discovery) for additional tissue grinding and then was carried to a 15 mL tube and centrifuged at 350 g for 10 min at room temperature. Cell sediment was then suspended in 1 ml of 70% isotonic Percoll solution. 1 ml of 50% Percoll solution was gently layered on top of the 70% layer, and 1 ml of PBS solution was then layered on top of the 50% Percoll layer. Density gradient was centrifuged for 40 min at 1200 g. After centrifugation, the layer at the interface between the 70% and 50% Percoll phases containing highly enriched microglia/macrophage was aspirated and cells were washed twice in PBS by centrifugation (Frank et al., 2006). Purity of isolated microglia/macrophage fraction was examined by flow cytometry using fluorescein isothiocyanate (FITC) mouse anti-rat CD11b (BD Pharmingen™) and phycoerythrin (PE) mouse anti-rat CD45 (BD Pharmingen™). The proportion of CD11b + $CD45^+$ cells was 88.9 ± 3.7%. Cell viability was determined by Trypan blue exclusion test. The proportion of viable cells was ≥93%.

2.8. Phagocyte metabolic profile assessment

Phagocyte metabolic profile was characterized by their phagocytic activity, oxidative metabolism, and phenotypic marker expression, which were examined by flow cytometry. Phagocytic activity was detected as described earlier (Rudyk et al., 2018). FITC-labeled thermally inactivated cells of *Staphylococcus aureus* Cowan I (collection of the Department of Microbiology and Immunology, ESC "Institute of Biology and Medicine" of Taras Shevchenko National University of Kyiv) were used as a phagocytosis object. $2x10^5$ microglia/macrophage cells were incubated at 37 °C for 30min with bacterial cells (5 μL of the stock suspension of FITC–labeled *S. aureus* at a concentration of 1×10^7 cells/mL). Phagocytosis was stopped by adding a 'stop' solution (PBS with 0.02% EDTA and 0.04% paraformaldehyde). Data are presented as the phagocytosis index (PhI) that representing the mean fluorescence per one phagocytic cell (ingested bacteria by one cell), and as phagocytosis percentage (PP) (percentage of cells emitting fluorescence). The phagocyte oxidative metabolism was examined using 2′7′-dichlorodihydrofluorescein diacetate (H2DCFDA, Invitrogen) as described previously (Rudyk et al., 2018). Reactivity reserve of the oxidative metabolism was characterized by the modulation coefficient (MC). MC was determined after the treatment of cell samples with phorbol 12-myristate 13-acetate (PMA) (protein kinase C activator, which has the ability to augment phagocyte oxidative metabolism) (Jin et al., 2021) *in vitro* and was calculated by the formula: MC = ((S–B) / B) × 100, where S − level of reactive oxygen species (ROS) generated after treatment with PMA *in vitro*; B − ROS value of untreated cells (basal value).

For phagocyte phenotyping, FITC-labeled anti-CD86, PE-labeled anti-CD80, and Alexa Fluor 647-labeled anti-CD206 antibodies (Becton Dickinson, Pharmingen, USA) were used. Results were assessed using FACSCalibur flow cytometer and CellQuest software (Becton Dickinson, USA).

2.9. Statistical analysis

All data are presented as mean ± SD. Data were tested using the Kolmogorov–Smirnov test for a normal distribution before other statistical tests. Statistical differences were calculated using ANOVA with Tukey's post-hoc test for multiple comparisons, and a two tailed *t*-test and non-parametric Mann-Whitney *U* test for single comparisons. Differences were considered significant at $p < 0.05$. Spearman correlation test was used to determine the statistical relationships between the values of measured microglia/macrophage metabolic characteristics and systemic inflammation marker values. A 2-tailed $p \leq 0.05$ was considered statistically significant.

3. Results

3.1. Behavioral features and DN loss in rats with 6-OHDA- and LPS-induced PD

The administration of both 6-OHDA and LPS was effective to cause brain injury as ascertained by the results of behavioral testing. Apomorphine test was used for comparative assessing the extent of the DN lesion. In 6-OHDA-lesioned rats, contralateral rotational rate was 7.6 rpm on day 8 after the surgery, indicating ≥80% DN damage and reflecting acute severe unilateral neurodegeneration (Fig. 1A). One week later, rotation rate in these animals came up 11.4 rpm, indicating progressive DN death. In LPS-lesioned group, contralateral rotation rate was 0.8 rpm 7 days, and 1.2 rpm 14 days after the endotoxin introduction, indicating moderate but progressive DN loss. Our results concord with the data of Eidson et al. (2017), which reported moderate progressive decrease in dopamine levels (≤50%) in rats after intrastriatal LPS injection. DN loss in lesioned rats was additionally confirmed by the TH immunostaining, which revealed ~60% decrease of TH-positive neurons in rats with LPS-PD and ~80% decrease in animals with 6-OHDA-PD (Fig. 1B–F).

The open-field test was used to assess physiological and psychosocial status of animals with both PD models. Ambulatory activity in 6-OHDA-lesioned animals was quite similar to those in LPS-lesioned rats. Significant decreases in total distance traveled: by 36% in 6-OHDA-lesioned rats and by 38% - in LPS-lesioned ones (Fig. 1G), and the number of rearing: by 59% and by 31% correspondingly (Fig. 1H) were registered in both model groups as compared to their sham-operated counterparts. The number of grooming was more reduced in rats with 6-OHDA-PD: by 27% vs 1% in animals with LPS-PD (Fig. 1I). The number of defecations in the session was also decreased in lesioned rats: by 28,2% in animals with 6-OHDA-PD and by 19.2% in LPS-lesioned ones as compared to control groups (Fig. 1J), indicating gastrointestinal malfunction with reduced colonic contractions, which is inherent in PD patients and rodents with experimental hemiparkinsonism (Minalyan et al., 2019). As for anxiety, the number of entries to the center of the arena was reduced in all lesioned animals on average by 1.3 times (Fig. 1K), latency to start the movement was increased in 6-OHDA lesioned rats by 4 times (Fig. 1L). This along with increased frequency of defecation (number of defecations per total distance traveled, Fig. 1M) indicates anxiety-like behavior in rats from both PD groups.

3.2. Metabolic characteristics of microglia/macrophages in rats with 6-OHDA- and LPS-induced PD: similarities and differences

Motor impairment and anxiety-like behavior in 6-OHDA- and LPS-

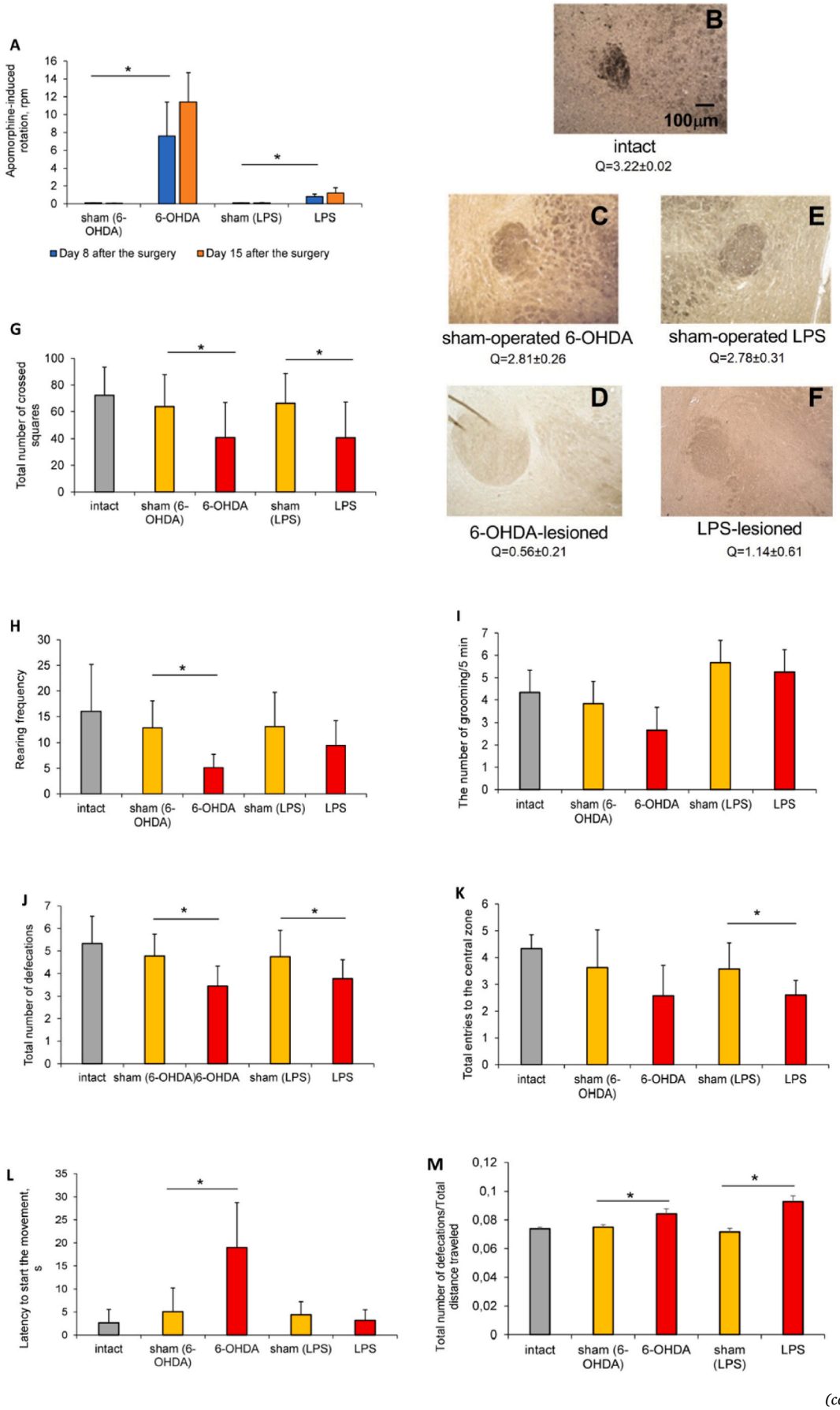

(caption on next page)

Fig. 1. Behavioral characteristics and dopaminergic neuron loss in rats with 6-OHDA- and LPS-induced Parkinson's disease. A – apomorphine test; B–F – representative immunohistochemical images of the TH-positive neurons (brown) in the midbrain of the 6-OHDA-PD (C, D) and LPS-PD (E, F) experimental groups (Quick scores (Q) under the images, calculated by multiplying the percentage of positive cells (P) by the intensity (I) and presented as: Q = P x I, are shown), magnification x50; G - total distance traveled; H - number of rearing; I - number of grooming; J – number of defecations in the session; K – number of entries to the center of the arena; L – latency to start the movement; M - frequency of defecation (number of defecations per total distance traveled). Data are presented as mean ± SD. Data from intact, sham-operated and lesioned animals were compared using ANOVA with Tukey post-hoc test. * - differences were considered to be significant when $P < 0.05$. (For interpretation of the references to colour in this figure legend, the reader is referred to the Web version of this article.)

lesioned rats were associated with slightly different metabolic profile of the microglia/macrophage population at the time point of the experiment cessation.

Phagocytic activity. Numerous studies specify a dysregulation (either up or downregulation) of microglia phagocytic activity as a prominent event in the PD pathophysiology (Janda et al., 2018; Ho, 2019). In our experiments, fraction of phagocytizing microglia/macrophage cells (PP) in 6-OHDA-lesioned rats was 1.4 times lower as compared to sham-operated animals and almost 3 times lower than that in intact animals (Fig. 2A). Whereas, percentage of phagocytizing microglia/macrophage cells (PP values) in LPS-lesioned animals didn't differ significantly from that in animals from control groups (Fig. 2A). The intensity of *S. aureus* phagocytosis (PhI) was reduced in both 6-OHDA- (by 1.2 times as compared to sham-operated animals and by 2.5 times in comparison with intact rats) and LPS-lesioned animals, but to the lesser extent: by 1.5 times as compared to intact rats (Fig. 2B).

Oxidative metabolism. Constitutive ROS generation is inherent in many cells including phagocytes considering their essential roles in signal transduction, cell differentiation, and gene expression (Canton et al., 2021). In phagocyte polarized activation, increased ROS generation is regarded as a metabolic marker of their pro-inflammatory functional skew (Jurga et al., 2020). In our experiments, baseline ROS generation by microglia/macrophage cells in lesioned rats from both models didn't differ significantly from that in control animals (Fig. 2C). In addition to the assessment of baseline ROS generation, we also examined the reactivity reserve of this phagocyte function (the remaining capacity of a cell to fulfill given metabolic activity under stress) after the treatment with PMA *in vitro*. Reactivity reserve was characterized by MC. Positive value of MC (see Materials and Methods) means the presence of reactivity reserve in analyzed cell population, whereas zero and/or negative value can evidence the maximum degree of the activation of the given function and lack of reactivity reserve or exhaustion of oxygen metabolism (Kanyilmaz et al., 2013). In animals from control groups, microglia/macrophage cell treatment with PMA *in vitro* resulted in boosted ROS generation (by 1.9 times on average), whereas it failed to boost their oxidative metabolism in lesioned rats from both models.

Phenotypic markers of the polarized activation. CD80 and CD86 are co-stimulatory molecules, which are necessary for antigen presentation and T cell activation. CD80 is expressed by both resting and activated resident microglial cells, whereas CD86 is expressed by only activated resident and recruited microglial cells (Böttcher et al., 2019). Upregulated expression of CD80/86 is considered as a marker of pro-inflammatory (M1) microglia/macrophage metabolic shift (Jurga et al., 2020). In our experiments, a fraction of CD80/86 positive cells in microglia/macrophage population from 6-OHDA-lesioned rats was 3.6 times lower than that in animals from control groups (Fig. 2D), whereas in LPS-lesioned rats, percentage of these cells was significantly (by 1.85 times) higher than that in intact animals and 4 times higher as compared with sham-operated rats (Fig. 2D). The levels of CD80/86 expression by microglia/macrophage cells from rats with both models were comparable to those in control animals (Fig. 2E). CD206 (mannose receptor C-type 1) is constitutively expressed by all macrophages, including resident microglial cells. It is a scavenger receptor binding both endogenous glycans (associated with tissue damage or apoptotic cell death) and microorganism sugars (Feinberg et al., 2021). CD206 ligation mostly produces anti-inflammatory responses, and therefore upregulation of CD206 expression is considered as a marker of anti-inflammatory phagocyte polarized activation (Jurga et al., 2020). In addition, microglia/macrophage population from 6-OHDA-lesioned rats was characterized by the increased fraction of CD206 positive cells (by 1.92 times as compared to intact animals and by 1.56 in comparison with values of sham-operated rats), the levels of CD206 surface expression didn't differ in lesioned and control animals (Fig. 2E). In LPS-lesioned rats, neither the percentage of CD206 positive microglia/macrophage cells, nor the level of CD206 surface expression differed in lesioned and control animals (Fig. 2D and E).

3.3. Systemic inflammatory markers in rats with 6-OHDA- and LPS-induced PD, and their association with microglia activation

As mentioned above, activated microglia contributes to the blood-brain barrier (BBB) impairment and promotes spread of inflammatory events to the periphery (Huang et al., 2021). We hypothesized that different features of microglia activation would correlate with dissimilar peripheral inflammatory changes. For testing the assumption, six most commonly used systemic inflammatory indices were exploited: NLR, dNLR, LMR, PLR, SIRI and SII (Table 1). NLR is a very sensitive and most commonly used indicator of systemic inflammation, which mirrors coupling and antagonism between innate and adaptive immunity in the course of various pathological states including neurodegenerative diseases (Zahorec, 2021). In 6-OHDA-lesioned rats, NLR values were 1.7 times lower than in intact animals, and moderately lower as compared to sham-operated animals. By contrast, NLR values in LPS-lesioned rats were almost twice as high as in control animals. dNLR is considered as more sensitive biomarker for systemic inflammation as compared to NLR, since it reflects the release of undifferentiated neutrophils and monocytes in a proinflammatory environment (Citu et al., 2022). Values of this marker were also increased in rats with LPS-PD as compared with their control counterparts (by 2.2 times on average), whereas dNLR values of 6-OHDA-lesioned animals didn't differ from those in control animals. LMR reflects involvement of mononuclear inflammatory cells (monocytes) in systemic inflammation (Nissen et al., 2019). In our experiments, LMR values in rats with 6-OHDA-PD were almost twice as low as in control animals, whereas in rats with LPS-PD - didn't differ significantly from those in control animals. PLR is a marker indicating changes in platelet and lymphocyte counts caused by SI with prothrombotic state (Madetko et al., 2022). PLR values in the group LPS-PD were 1.7 times higher as compared to those in intact animals, and 1.5 times higher than in their sham-operated counterparts. In 6-OHDA-PD model, PLR values didn't differ in lesioned and control animals. SIRI combines neutrophil, monocyte and lymphocyte count, mirrors the host immune and inflammation balance, thereby reflecting the state of immunodeficiency or immune exhausting. SII combines neutrophil, platelet and lymphocyte count and represents more integral index of systemic inflammation with prothrombotic component as compared to PLR. In our experiments, there were no significant differences between the values of SIRI in lesioned and control animals in both models. SII values in 6-OHDA-lesioned rats were moderately lower than those in control animals, whereas in LPS-lesioned rats these indices were more than 2 times higher as compared with control animals. Correlation analysis revealed associations between the proportion of CD80/86 cells in microglia/macrophage population and several SI indices in lesioned animals of both models. Surprisingly, these associations were opposite in 6-OHDA-PD and LPS-PD (Fig. 3A–H). In animals with 6-OHDA-PD moderate negative correlations were found between the proportion of

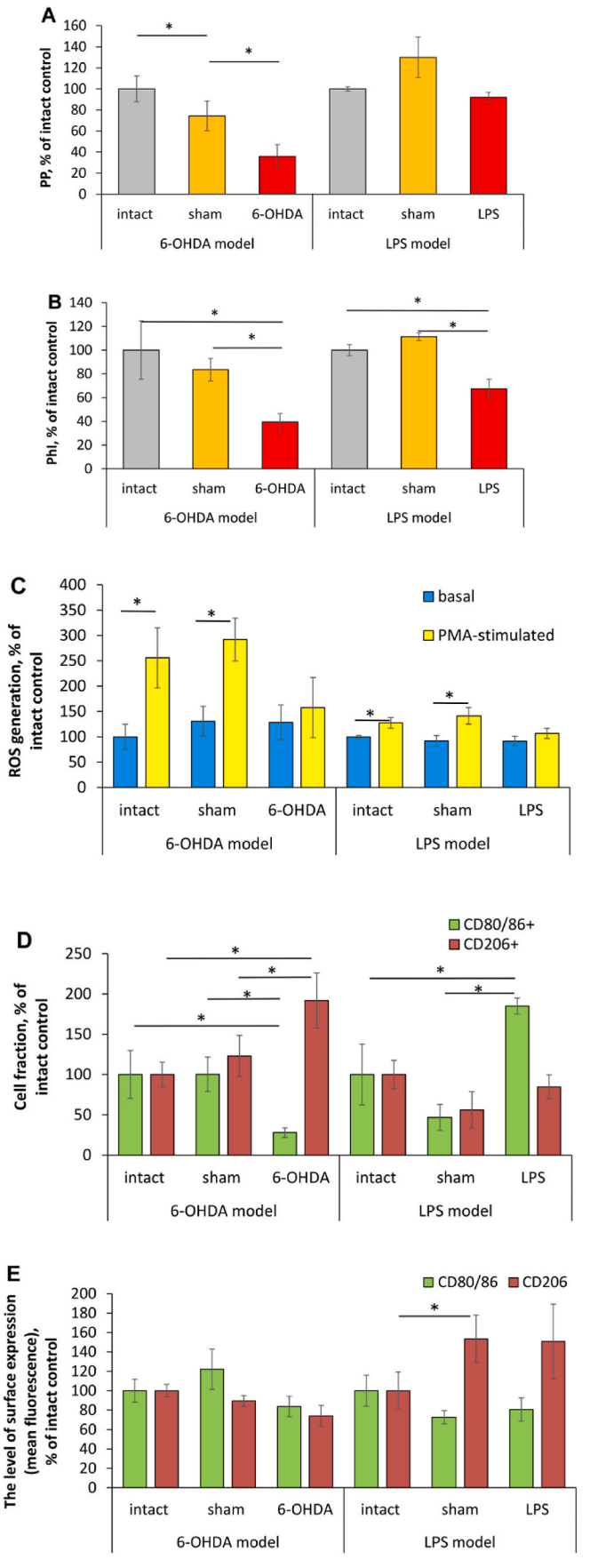

(caption on next column)

Fig. 2. Metabolic characteristics of microglia/macrophages in rats with 6-OHDA-induced and LPS-induced Parkinson's disease. A – phagocytosis percentage (see Materials and Methods); B – phagocytosis index; C – basal and PMA-stimulated ROS generation; D – phenotypic marker expression, the percentage of positive cells; E – phenotypic marker expression, expression level (mean fluorescence intensity). Data are presented as mean ± SD. Data from intact, sham-operated and lesioned animals were compared using ANOVA with Tukey post-hoc test. * - differences were considered to be significant when $P < 0.05$. Measurements in samples after the treatment with PMA *in vitro* were compared with untreated samples using a two tailed T-test, # - $P < 0.05$ versus corresponding untreated control.
PD, Parkinson's disease; PP, phagocytosis percentage; PhI, phagocytosis index; ROS, reactive oxygen species.

CD80/86 cells and NLR and SII ($r_s = -0.61$ and -0.65 correspondingly) (Fig. 3A and G). Whereas in rats with LPS-PD, strong positive correlation was detected between the proportion of CD80/86 cells and NLR, PLR and SII ($r_s = 0.71$, 0.78 and 0.74 correspondingly) (Fig. 3B, F and H).

4. Discussion

In the current study, we conducted comparative evaluation of behavioral features, DN loss, and, most importantly, activation patterns of microglia/macrophage population and their association with SI manifestation in rats with 6-OHDA- and LPS-induced PD. We found comparable impairment of ambulatory activity, gastrointestinal dysfunction, and anxiety-like behavior in both models. At the same time, DN loss was significantly more pronounced in 6-OHDA-lesioned rats as compared to LPS-lesioned animals. In doing so, we observed more explicit pro-inflammatory metabolic shift in microglia/macrophage cells in rats with LPS-PD (as evidenced by significantly increase of CD80/86 positive cell fraction). It suggests that behavioral abnormalities in 6-OHDA-lesioned rats may be primarily stipulated by DN damage as a result of selective toxic effect of 6-OHDA (García-Revilla et al., 2022), whereas motor and non-motor symptoms in LPS-lesioned animals may be foremost associated with more pronounced pro-inflammatory activation of the microglia/macrophage cell population. Our data are in agreement with findings of Parra et al. (2020), which revealed that 6-OHDA causes a high degree of DN loss, and a lower degree of microglia activation compared to LPS, as was evident by the analysis of microglia morphology. Nevertheless, animal treated with both toxins were characterized by comparable motor impairment in these experiments. In addition, our data support the allegation that PD can't be considered as a disease of DN exclusively, since multiple populations of neurons in multiple regions of the central and peripheral nervous system are affected in this disease (Giguère et al., 2018; Matschke et al., 2022).

Metabolic characteristics of microglia/macrophage population in 6-OHDA- and LPS-lesioned animals at the time of the experiment cessation (day 29 after the surgery) were identical in many respects: down regulated phagocytic activity alongside the prolonged activation of oxidative metabolism as ascertained by the absence of the reactivity reserve of this function, indicates pro-inflammatory functional skew in cells from rats with both PD models (Jurga et al., 2020). It is well documented that M1 polarized activation of phagocytes is accompanied by the continuous ROS generation and acquiring antigen-presenting ability, both of these functions followed by delayed phagosome maturation and progressive decrease in phagocytic activity (Tan et al., 2016; Yanuck, 2019). Nevertheless, we registered some important distinctions in the activation patterns of microglia/macrophage population in 6-OHDA- and LPS-induced PD. At the time of experiment cessation, the fraction of phagocytizing cells, as well as fraction of CD80/86-positive cells in microglia/macrophage population remained quite high in animals with LPS-PD. It can indicate ongoing neuroinflammation in animals with this model even 28 days after the disease initiation. This assumption is in line with data presenting by Janda et al. (2018), according to which pro-inflammatory and phagocytic TREM2-positive microglia with

Table 1
Systemic inflammation markers in rats with 6-OHDA-induced and LPS-induced Parkinson's disease. Data are presented as mean ± SD. * - P < 0.05 as compared to intact animals; # - P < 0.05 as compared to sham-operated animals (ANOVA with Tukey post-hoc test). dNLR, Derived neutrophil to lymphocyte ratio; LMR, Lymphocyte to monocyte ratio; NLR, Neutrophil to lymphocyte ratio; PD, Parkinson's disease; PLR, platelet to lymphocyte ratio; SII, Systemic immune inflammation index; SIRI, Systemic inflammatory response index.

Systemic inflammation marker	6 –OHDA-induced PD			LPS-induced PD		
	Intact animals, n = 10	sham-operated animals, n = 10	6 –OHDA-lesioned animals, n = 10	Intact animals, n = 10	sham-operated animals, n = 10	LPS-lesioned animals, n = 10
NLR	0.35 ± 0.07	0.27 ± 0.12	0.21 ± 0.06*	0.25 ± 0.09	0.29 ± 0.09	0.54 ± 0.12*#
dNLR	0.41 ± 0.05	0.34 ± 0.12	0.32 ± 0.18	0.23 ± 0.07	0.25 ± 0.07	0.53 ± 0.14*#
LMR	7.61 ± 2.66	8,45 ± 2.28	4.39 ± 0.82*#	8.39 ± 1.78	6.78 ± 2.28	8.27 ± 2.45
PLR	25.53 ± 6.57	28.64 ± 9.25	27.72 ± 15.25	29.54 ± 6.91	34.58 ± 7.52	51.81 ± 7.84*#
SIRI	0.20 ± 0.08	0.13 ± 0.05	0.19 ± 0.11	0.11 ± 0.04	0.12 ± 0.09	0.21 ± 0.09
SII	33.73 ± 9.09	32.852 ± 8.04	23.52 ± 2.04*	37.24 ± 8.97	41.91 ± 7.83	77.58 ± 4.53*#

increased Major Histocompatibility Complex (MHC) II and costimulatory molecules expression are prevalent in PD patients, especially in late stages of the disease. In our microglia phagocytosis assay we used bacterial cells. TREM2 (Triggering Receptor Expressed on Myeloid cells) participates in both phagocytosis of apoptotic neurons and a wide variety of bacteria by microglia (Tremblay et al., 2019). By contrast, the fraction of phagocytizing cells in the microglia/macrophage population from 6-OHDA-lesioned rats was significantly decreased as compared with LPS-lesioned animals. Substantial decrease in the percentage of CD80/86-positive cells alongside the high proportion of CD206-positive cells were also registered in animals with 6-OHDA-PD. Altogether these data can evidence spontaneous resolution of the neuroinflammation in lesioned rats. Our assumption concord with numerous literature data, in which acute nature of 6-OHDA-induced PD with the potential for spontaneous neuroreparation and resolution of neuroinflammation are considered as one of the drawbacks of this model (Bezard et al., 2013; Jagmag et al., 2016; Okyere et al., 2021).

A further distinction between 6-OHDA- and LPS-PD models was in the manifestation of SI. Neuroinflammation with the involvement of microglia, as is known, creates vicious circle with SI, which gives PD chronic scope. Inflammatory mediators, produced by activated microglia enter the periphery and activate peripheral immunocytes followed by the appearance of systemic inflammation markers in blood (Lerche et al., 2022). Inflammatory mediators from peripheral immune cells in turn can enter the brain, either through neural or humoral pathways. Humoral pathway presupposes transporting these mediators with blood through the disturbed BBB. Neural pathway is associated with the transfer of peripheral pro-inflammatory signals through the autonomic nervous system (Ferrari and Tarelli, 2011). These inflammatory mediators, being transported to the brain, maintain and exacerbate neuroinflammation and neurodegeneration. Moreover, systemic inflammatory changes correlate with disease severity (Roy et al., 2021). CD80/86 positive microglial cells are considered as the main source of pro-inflammatory mediators including Th1 cytokines, which are responsible for spreading neuroinflammation to the periphery (Jurga et al., 2020). In our experiments, the values of systemic inflammatory indices, which reflect most precisely persistent SI (NLR, dNLR, PLR and SII) (Citu et al., 2022) were increased as compared to the control only in LPS-lesioned rats, indicating that systemic spread of neuroinflammation as a sign of crosstalk between central and peripheral immune system is characteristic of this model, in contrast to 6-OHDA-PD. Systemic inflammatory indices correlated with proportions of CD80/86+ cells in microglia/macrophage populations in both models but in different way. The proportion of CD80/86+ microglial cells was found to be positively correlated with the NLR, PLR and SII values in rats with LPS-PD. One can suppose that these M1-polarized phagocytes with properties of antigen-presenting cells are associated with spreading of the inflammation to the periphery in this model. In rats with 6-OHDA-PD, proportion of CD80/86+ microglial cells correlated negatively with values of SI indices. This phenomenon may be explained by dual role of B7 family members in the immune response regulation. Namely, CD80/86+ cells may belong to both M1-polarized immunostimulatory myeloid cells and myeloid-derived suppressor cells (MDSC) involved in the resolution of inflammation (Collins et al., 2005). One can suppose, that in case of 6-OHDA-PD, CD80/86+ microglial cells, the number of which correlated negatively with SI manifestation, belong to MDSC.

Several limitations of this study must be noted. Differences in the patterns of microglia/macrophage activation in 6-OHDA and LPS PD models must be examined over time after the toxins introduction to achieve a deeper comprehension of the phenomenon. We used limited number of metabolic characteristics to assess activation pattern of microglia/macrophage population, and additional features including arginine metabolism and cytokine profile must be evaluated to strengthen our findings. Deep insight into reasons for the distinctions in the activation patterns of complex microglia/macrophage population requires separate evaluation of resident microglial cells and recruited monocyte-derived macrophages. E.g., macrophages from the periphery can be differentiated from the resident microglial cells by their expression of Tmem119, CD44 (Segal and Giger, 2016; Jurga et al., 2020) and CD169 (Jurga et al., 2020).

5. Conclusions

In summary, our results indicate that comparable neuroinflammation is induced in both LPS- and 6-OHDA-PD models. However, the mechanisms seem to be different considering that these disease-initiating substances induce polarized activation of complex microglia/macrophages population using different receptors and pathways, thereby affecting PD modeling, including local and systemic inflammation development, in different way. Phenomenon of strong correlation between neuroinflammation and SI features in LPS-PD deserves further scientific analysis in terms of using this model for studying crosstalk between local and systemic inflammatory responses in the disease pathogenesis and for searching new therapeutic targets. Future experiments aiming to study the correlation between indices of SI and tissue-resident and recruited CD80/86 positive cell number separately will contribute to more precise finding of aforementioned therapeutic targets for anti-inflammatory agents in the complex PD treatment.

Funding sources

This research did not receive any specific grant from funding agencies in the public, commercial, or not-for-profit sectors.

Declaration of competing interest

The authors declare that they have no known competing financial interests or personal relationships that could have appeared to influence the work reported in this paper.

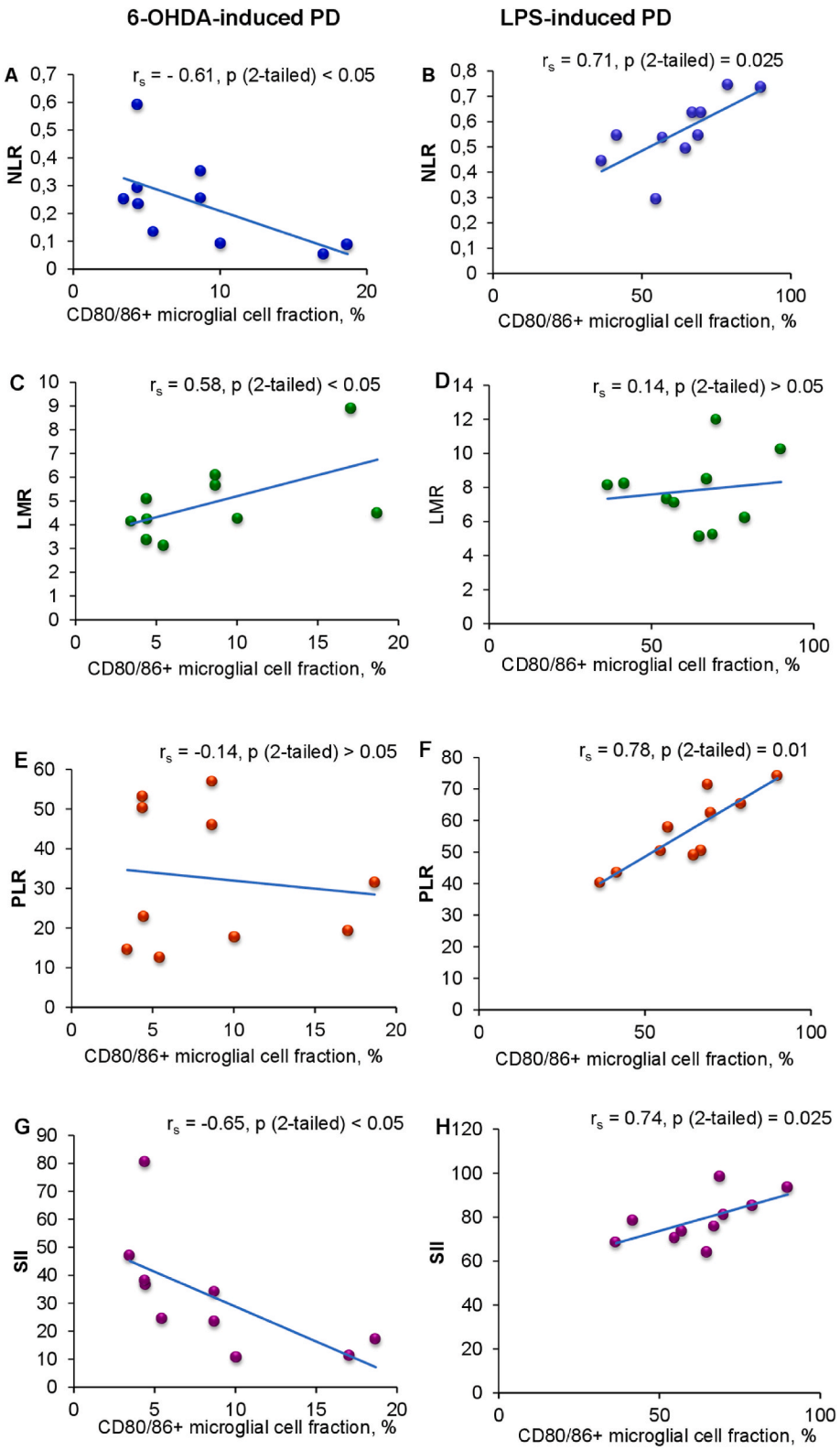

Fig. 3. Correlations between the percentage of CD80/86 positive cells in microglia/macrophage population and systemic inflammation indices in rats with 6-OHDA-induced (A, C, E, G) and LPS-induced (B, D, F, H) Parkinson's disease. LMR, lymphocyte to monocyte ratio; NLR, neutrophil to lymphocyte ratio (see Materials and Methods); PD, Parkinson's disease; PLR, platelet to lymphocyte ratio; SII, systemic immune inflammation index.

Data availability

Data will be made available on request.

References

Abellanas, M.A., Zamarbide, M., Basurco, L., Luquin, E., Garcia-Granero, M., Clavero, P., San Martin-Uriz, P., Vilas, A., Mengual, E., Hervas-Stubbs, S., Aymerich, M.S., 2019. Midbrain microglia mediate a specific immunosuppressive response under

inflammatory conditions. J. Neuroinflammation 16 (1), 233. https://doi.org/10.1186/s12974-019-1628-8.
Agirman, G., Yu, K.B., Hsiao, E.Y., 2021. Signaling inflammation across the gut-brain axis. Science 374 (6571), 1087–1092. https://doi.org/10.1126/science.abi6087.
Araújo, B., Caridade-Silva, R., Soares-Guedes, C., Martins-Macedo, J., Gomes, E.D., Monteiro, S., Teixeira, F.G., 2022. Neuroinflammation and Parkinson's disease-from neurodegeneration to therapeutic opportunities. Cells 11 (18), 2908. https://doi.org/10.3390/cells11182908.
Bezard, E., Yue, Z., Kirik, D., Spillantini, M.G., 2013. Animal models of Parkinson's disease: limits and relevance to neuroprotection studies. Mov. Disord. 28 (1), 61–70. https://doi.org/10.1002/mds.25108.
Blandini, F., Levandis, G., Bazzini, E., Nappi, G., Armentero, M.T., 2007. Time-course of nigrostriatal damage, basal ganglia metabolic changes and behavioural alterations following intrastriatal injection of 6-hydroxydopamine in the rat: new clues from an old model. Eur. J. Neurosci. 25 (2), 397–405. https://doi.org/10.1111/j.1460-9568.2006.05285.x.
Böttcher, C., Schlickeiser, S., Sneeboer, M.M.A., Kunkel, D., Knop, A., Paza, E., Fidzinski, P., Kraus, L., Snijders, G.J.L., Kahn, R.S., Schulz, A.R., Mei, H.E., NBB-Psy Hol, E.M., Siegmund, B., Glauben, R., Spruth, E.J., de Witte, L.D., Priller, J., 2019. Human microglia regional heterogeneity and phenotypes determined by multiplexed single-cell mass cytometry. Nat. Neurosci. 22, 78–90. https://doi.org/10.1038/s41593-018-0290-2.
Canton, M., Sánchez-Rodríguez, R., Spera, I., Venegas, F.C., Favia, M., Viola, A., Castegna, A., 2021. Reactive oxygen species in macrophages: sources and targets. Front. Immunol. 12, 734229 https://doi.org/10.3389/fimmu.2021.734229.
Chen, L., Wang, Y., Huang, J., Hu, B., Huang, W., 2022. Identification of immune-related hub genes in Parkinson's disease. Front. Genet. 13, 914645 https://doi.org/10.3389/fgene.2022.914645.
Cherry, J.D., Olschowka, J.A., O'Banion, M.K., 2014. Are "resting" microglia more "m2. Front. Immunol. 5, 594. https://doi.org/10.3389/fimmu.2014.00594.
Citu, C., Gorun, F., Motoc, A., Sas, I., Gorun, O.M., Burlea, B., Tuta-Sas, I., Tomescu, L., Neamtu, R., Malita, D., Citu, I.M., 2022. The predictive role of NLR, d-NLR, MLR, and SIRI in COVID-19 mortality. Diagnostics 12 (1), 122. https://doi.org/10.3390/diagnostics12010122.
Collins, M., Ling, V., Carreno, B.M., 2005. The B7 family of immune-regulatory ligands. Genome Biol. 6 (6), 223. https://doi.org/10.1186/gb-2005-6-6-223.
Dogra, N., Mani, R.J., Katare, D.P., 2022. The gut-brain Axis: two ways signaling in Parkinson's disease. Cell. Mol. Neurobiol. 42 (2), 315–332. https://doi.org/10.1007/s10571-021-01066-7.
Eidson, L.N., Kannarkat, G.T., Barnum, C.J., Chang, J., Chung, J., Caspell-Garcia, C., Taylor, P., Mollenhauer, B., Schlossmacher, M.G., Ereshefsky, L., Yen, M., Kopil, C., Frasier, M., Marek, K., Hertzberg, V.S., Tansey, M.G., 2017. Candidate inflammatory biomarkers display unique relationships with alpha-synuclein and correlate with measures of disease severity in subjects with Parkinson's disease. J. Neuroinflammation 14 (1), 164. https://doi.org/10.1186/s12974-017-0935-1.
Feinberg, H., Jégouzo, S.A.F., Lasanajak, Y., Smith, D.F., Drickamer, K., Weis, W.I., Taylor, M.E., 2021. Structural analysis of carbohydrate binding by the macrophage mannose receptor CD206. J. Biol. Chem. 296, 100368 https://doi.org/10.1016/j.jbc.2021.100368.
Ferrari, C.C., Tarelli, R., 2011. Parkinson's disease and systemic inflammation. Parkinsons Dis 2011, 436813. https://doi.org/10.4061/2011/436813.
Frank, M.G., Wieseler-Frank, J.L., Watkins, L.R., Maier, S.F., 2006. Rapid isolation of highly enriched and quiescent microglia from adult rat hippocampus: immunophenotypic and functional characteristics. J. Neurosci. Methods 151 (2), 121–130. https://doi.org/10.1016/j.jneumeth.2005.06.026.
García-Revilla, J., Herrera, A.J., de Pablos, R.M., Venero, J.L., 2022. Inflammatory animal models of Parkinson's disease. J. Parkinsons Dis. 12 (s1), S165–S182. https://doi.org/10.3233/JPD-213138.
Gaviglio, E.A., Peralta Ramos, J.M., Arroyo, D.S., Bussi, C., Iribarren, P., Rodriguez-Galan, M.C., 2022. Systemic sterile induced-co-expression of IL-12 and IL-18 drive IFN-γ-dependent activation of microglia and recruitment of MHC-II-expressing inflammatory monocytes into the brain. Int. Immunopharm. 105, 108546 https://doi.org/10.1016/j.intimp.2022.108546.
Gelders, G., Baekelandt, V., Van der Perren, A., 2018. Linking neuroinflammation and neurodegeneration in Parkinson's disease. J. Immunol. Res. 2018, 4784268 https://doi.org/10.1155/2018/4784268.
Giguère, N., Burke Nanni, S., Trudeau, L.E., 2018. On cell loss and selective vulnerability of neuronal populations in Parkinson's disease. Front. Neurol. 9, 455. https://doi.org/10.3389/fneur.2018.00455.
Gopinath, A., Mackie, P., Hashimi, B., Buchanan, A.M., Smith, A.R., Bouchard, R., Shaw, G., Badov, M., Saadatpour, L., Gittis, A., Ramirez-Zamora, A., Okun, M.S., Streit, W.J., Hashemi, P., Khoshbouei, H., 2022. DAT and TH expression marks human Parkinson's disease in peripheral immune cells. NPJ Parkinsons Dis 8 (1), 72. https://doi.org/10.1038/s41531-022-00333-8.
Grassivaro, F., Martino, G., Farina, C., 2021. The phenotypic convergence between microglia and peripheral macrophages during development and neuroinflammation paves the way for new therapeutic perspectives. Neural Regen. Res. 16 (4), 635–637. https://doi.org/10.4103/1673-5374.295272.
Gundersen, V., 2021. Parkinson's disease: can targeting inflammation Be an effective neuroprotective strategy? Front. Neurosci. 14, 580311 https://doi.org/10.3389/fnins.2020.580311.
Haruwaka, K., Ikegami, A., Tachibana, Y., Ohno, N., Konishi, H., Hashimoto, A., Matsumoto, M., Kato, D., Ono, R., Kiyama, H., Moorhouse, A.J., Nabekura, J., Wake, H., 2019. Dual microglia effects on blood brain barrier permeability induced by systemic inflammation. Nat. Commun. 10 (1), 5816. https://doi.org/10.1038/s41467-019-13812-z.
Ho, M.S., 2019. Microglia in Parkinson's disease. Adv. Exp. Med. Biol. 1175, 335–353. https://doi.org/10.1007/978-981-13-9913-8_13.
Hoban, D.B., Connaughton, E., Connaughton, C., Hogan, G., Thornton, C., Mulcahy, P., Moloney, T.C., Dowd, E., 2013. Further characterisation of the LPS model of Parkinson's disease: a comparison of intra-nigral and intra-striatal lipopolysaccharide administration on motor function, microgliosis and nigrostriatal neurodegeneration in the rat. Brain Behav. Immun. 27 (1), 91–100. https://doi.org/10.1016/j.bbi.2012.10.001.
Hourfar, H., Aliakbari, F., Aqdam, S.R., Nayeri, Z., Bardania, H., Otzen, D.E., Morshedi, D., 2023. The impact of α-synuclein aggregates on blood-brain barrier integrity in the presence of neurovascular unit cells. Int. J. Biol. Macromol. 229, 305–320. https://doi.org/10.1016/j.ijbiomac.2022.12.134.
Hu, B., Yang, X.R., Xu, Y., Sun, Y.F., Sun, C., Guo, W., Zhang, X., Wang, W.M., Qiu, S.J., Zhou, J., Fan, J., 2014. Systemic immune-inflammation index predicts prognosis of patients after curative resection for hepatocellular carcinoma. Clin. Cancer Res. 20 (23), 6212–6222. https://doi.org/10.1158/1078-0432.CCR-14-0442.
Huang, X., Hussain, B., Chang, J., 2021. Peripheral inflammation and blood-brain barrier disruption: effects and mechanisms. CNS Neurosci. Ther. 27 (1), 36–47. https://doi.org/10.1111/cns.13569.
Jagmag, S.A., Tripathi, N., Shukla, S.D., Maiti, S., Khurana, S., 2016. Evaluation of models of Parkinson's disease. Front. Neurosci. 9, 503. https://doi.org/10.3389/fnins.2015.00503.
Janda, E., Boi, L., Carta, A.R., 2018. Microglial phagocytosis and its regulation: a therapeutic target in Parkinson's disease? Front. Mol. Neurosci. 11, 144. https://doi.org/10.3389/fnmol.2018.00144.
Jin, Y., Dixon, B., Jones, L., Gorbet, M., 2021. The differential reactive oxygen species production of tear neutrophils in response to various stimuli in vitro. Int. J. Mol. Sci. 22 (23), 12899 https://doi.org/10.3390/ijms222312899.
Jurga, A.M., Paleczna, M., Kuter, K.Z., 2020. Overview of general and discriminating markers of differential microglia phenotypes. Front. Cell. Neurosci. 14, 198. https://doi.org/10.3389/fncel.2020.00198.
Kanyilmaz, S., Hepguler, S., Atamaz, F.C., Gokmen, N.M., Ardeniz, O., Sin, A., 2013. Phagocytic and oxidative burst activity of neutrophils in patients with spinal cord injury. Arch. Phys. Med. Rehabil. 94 (2), 369–374. https://doi.org/10.1016/j.apmr.2012.09.015.
Lama, J., Buhidma, Y., Fletcher, E.J.R., Duty, S., 2021. Animal models of Parkinson's disease: a guide to selecting the optimal model for your research. Neuronal Signal 5 (4), NS20210026. https://doi.org/10.1042/NS20210026.
Lashgari, N.A., Roudsari, N.M., Momtaz, S., Sathyapalan, T., Abdolghaffari, A.H., Sahebkar, A., 2021. The involvement of JAK/STAT signaling pathway in the treatment of Parkinson's disease. J. Neuroimmunol. 361, 577758 https://doi.org/10.1016/j.jneuroim.2021.577758.
Lee, E., Eo, J.C., Lee, C., Yu, J.W., 2021a. Distinct features of brain-resident macrophages: microglia and non-parenchymal brain macrophages. Mol. Cell. 44 (5), 281–291. https://doi.org/10.14348/molcells.2021.0060.
Lee, J.W., Chun, W., Lee, H.J., Kim, S.M., Min, J.H., Kim, D.Y., Kim, M.O., Ryu, H.W., Lee, S.U., 2021b. The role of microglia in the development of neurodegenerative diseases. Biomedicines 9 (10), 1449. https://doi.org/10.3390/biomedicines9101449.
Leite-Almeida, H., Almeida-Torres, L., Mesquita, A.R., Pertovaara, A., Sousa, N., Cerqueira, J.J., Almeida, A., 2009. The impact of age on emotional and cognitive behaviours triggered by experimental neuropathy in rats. Pain 144 (1–2), 57–65. https://doi.org/10.1016/j.pain.2009.02.024.
Lerche, S., Zimmermann, M., Wurster, I., Roeben, B., Fries, F.L., Deuschle, C., Waniek, K., Lachmann, I., Gasser, T., Jakobi, M., Joos, T.O., Schneiderhan-Marra, N., Brockmann, K., 2022. CSF and serum levels of inflammatory markers in PD: sparse correlation, sex differences and association with neurodegenerative biomarkers. Front. Neurol. 13, 834580 https://doi.org/10.3389/fneur.2022.834580.
MacMahon Copas, A.N., McComish, S.F., Fletcher, J.M., Caldwell, M.A., 2021. The pathogenesis of Parkinson's disease: a complex interplay between astrocytes, microglia, and T lymphocytes? Front. Neurol. 12, 666737 https://doi.org/10.3389/fneur.2021.666737.
Madetko, N., Migda, B., Alster, P., Turski, P., Koziorowski, D., Friedman, A., 2022. Platelet-to-lymphocyte ratio and neutrophil-tolymphocyte ratio may reflect differences in PD and MSA-P neuroinflammation patterns. Neurol. Neurochir. Pol. 56 (2), 148–155. https://doi.org/10.5603/PJNNS.a2022.0014.
Magistrelli, L., Contaldi, E., Vignaroli, F., Gallo, S., Colombatto, F., Cantello, R., Comi, C., 2022. Immune response modifications in the genetic forms of Parkinson's disease: what do we know? Int. J. Mol. Sci. 23 (7), 3476. https://doi.org/10.3390/ijms23073476.
Matschke, L.A., Komadowski, M.A., Stöhr, A., Lee, B., Henrich, M.T., Griesbach, M., Rinné, S., Geibl, F.F., Chiu, W.H., Koprich, J.B., Brotchie, J.M., Kiper, A.K., Dolga, A. M., Oertel, W.H., Decher, N., 2022. Enhanced firing of locus coeruleus neurons and SK channel dysfunction are conserved in distinct models of prodromal Parkinson's disease. Sci. Rep. 12 (1), 3180. https://doi.org/10.1038/s41598-022-06832-1.
Miao, Q., Chai, Z., Song, L.J., Wang, Q., Song, G.B., Wang, J., Yu, J.Z., Xiao, B.G., Ma, C. G., 2022. The neuroprotective effects and transdifferentiation of astrocytes into dopaminergic neurons of Ginkgolide K on Parkinson' disease mice. J. Neuroimmunol. 364, 577806 https://doi.org/10.1016/j.jneuroim.2022.577806.
Minalyan, A., Gabrielyan, L., Pietra, C., Taché, Y., Wang, L., 2019. Multiple beneficial effects of ghrelin agonist, HM01 on homeostasis alterations in 6-hydroxydopamine model of Parkinson's disease in male rats. Front. Integr. Neurosci. 13, 13. https://doi.org/10.3389/fnint.2019.00013.
Muzio, L., Viotti, A., Martino, G., 2021. Microglia in neuroinflammation and neurodegeneration: from understanding to therapy. Front. Neurosci. 15, 742065 https://doi.org/10.3389/fnins.2021.742065.

Nissen, S.K., Shrivastava, K., Schulte, C., Otzen, D.E., Goldeck, D., Berg, D., Møller, H.J., Maetzler, W., Romero-Ramos, M., 2019. Alterations in blood monocyte functions in Parkinson's disease. Mov. Disord. 34 (11), 1711–1721. https://doi.org/10.1002/mds.27815.

Öberg, M., Fabrik, I., Fabrikova, D., Zehetner, N., Härtlova, A., 2021. The role of innate immunity and inflammation in Parkinson's disease. Scand. J. Immunol. 93 (5), e13022 https://doi.org/10.1111/sji.13022.

Okyere, K.S., Zeng, C., Yue, D., Hu, Y., 2021. Neurotoxic mechanism and shortcomings of MPTP, 6-OHDA, rotenone and paraquat-induced Parkinson's disease animal models. Venoms Toxins 1 (1), 27–40. https://doi.org/10.2174/2666121701999201104163407.

Oliynyk, Zh, Rudyk, M., Svyatetska, V., Dovbynchuk, T., Tolstanova, G., Skivka, L., 2022. Systemic inflammation biomarkers in 6-OHDA- and LPS-induced Parkinson's disease in rats. Ukrainian Biochem. J. 94, 33–43. https://doi.org/10.15407/ubj94.01.033.

Parra, I., Martínez, I., Ramírez-García, G., Tizabi, Y., Mendieta, L., 2020. Differential effects of LPS and 6-OHDA on microglia's morphology in rats: implications for inflammatory model of Parkinson's disease. Neurotox. Res. 37 (1), 1–11. https://doi.org/10.1007/s12640-019-00104-z.

Pauletti, G., Dandekar, S., Rong, H., Ramos, L., Peng, H., Seshadri, R., Slamon, D.J., 2000. Assessment of methods for tissue-based detection of the HER-2/neu alteration in human breast cancer: a direct comparison of fluorescence in situ hybridization and immunohistochemistry. J. Clin. Oncol. 18 (21), 3651–6364. https://doi.org/10.1200/JCO.2000.18.21.3651.

Paxinos, G., Watson, C., 2007. The Rat Brain in Stereotaxic Coordinates, sixth ed. Academic Press, San Diego.

Rosadini, C.V., Kagan, J.C., 2017. Early innate immune responses to bacterial LPS. Curr. Opin. Immunol. 44, 14–19. https://doi.org/10.1016/j.coi.2016.10.005.

Roy, A., Mondal, B., Banerjee, R., Choudhury, S., Chatterjee, K., Dey, S., Kumar, H., 2021. Do peripheral immune and neurotrophic markers correlate with motor severity of Parkinson's disease? J. Neuroimmunol. 354, 577545 https://doi.org/10.1016/j.jneuroim.2021.577545.

Rudyk, M.P., Pozur, V.V., Voieikova, D.O., Hurmach, Y.V., Khranovska, N.M., Skachkova, O.V., Svyatetska, V.M., Fedorchuk, O.G., Skivka, L.M., Berehova, T.V., Ostapchenko, L.I., 2018. Sex-based differences in phagocyte metabolic profile in rats with monosodium glutamate-induced obesity. Sci. Rep. 8 (1), 5419. https://doi.org/10.1038/s41598-018-23664-0.

Segal, B.M., Giger, R.J., 2016. Stable biomarker for plastic microglia. Proc. Natl. Acad. Sci. U.S.A. 113 (12), 3130–3132. https://doi.org/10.1073/pnas.1601669113.

Sestakova, N., Puzserova, A., Kluknavsky, M., Bernatova, I., 2013. Determination of motor activity and anxiety-related behaviour in rodents: methodological aspects and role of nitric oxide. Interdiscipl. Toxicol. 6 (3), 126–135. https://doi.org/10.2478/intox-2013-0020.

Sevenich, L., 2018. Brain-resident microglia and blood-borne macrophages orchestrate central nervous system inflammation in neurodegenerative disorders and brain cancer. Front. Immunol. 9, 697. https://doi.org/10.3389/fimmu.2018.00697.

Smith, G.A., Heuer, A., Dunnett, S.B., Lane, E.L., 2012. Unilateral nigrostriatal 6-hydroxydopamine lesions in mice II: predicting l-DOPA-induced dyskinesia. Behav. Brain Res. 226 (1), 281–292. https://doi.org/10.1016/j.bbr.2011.09.025.

Su, R.J., Zhen, J.L., Wang, W., Zhang, J.L., Zheng, Y., Wang, X.M., 2018. Time-course behavioral features are correlated with Parkinson's disease associated pathology in a 6-hydroxydopamine hemiparkinsonian rat model. Mol. Med. Rep. 17 (2), 3356–3363. https://doi.org/10.3892/mmr.2017.8277.

Takata, F., Nakagawa, S., Matsumoto, J., Dohgu, S., 2021. Blood-brain barrier dysfunction amplifies the development of neuroinflammation: understanding of cellular events in brain microvascular endothelial cells for prevention and treatment of BBB dysfunction. Front. Cell. Neurosci. 15, 661838 https://doi.org/10.3389/fncel.2021.661838.

Talanov, S.A., Oleshko, N.N., Tkachenko, M.N., Sagach, V.F., 2006. Pharmacoprotective influences on different links of the mechanism underlying 6-hydroxydopamine-induced degeneration of nigro-striatal dopaminergic neurons. Neurophysiology 38 (2), 128–133. https://doi.org/10.1007/s11062-006-0035-9.

Tan, H.Y., Wang, N., Li, S., Hong, M., Wang, X., Feng, Y., 2016. The reactive oxygen species in macrophage polarization: reflecting its dual role in progression and treatment of human diseases. Oxid. Med. Cell. Longev. 2016, 2795090. https://doi.org/10.1155/2016/2795090.

Tansey, M.G., Wallings, R.L., Houser, M.C., Herrick, M.K., Keating, C.E., Joers, V., 2022. Inflammation and immune dysfunction in Parkinson disease. Nat. Rev. Immunol. 22 (11), 657–673. https://doi.org/10.1038/s41577-022-00684-6.

Tremblay, M.E., Cookson, M.R., Civiero, L., 2019. Glial phagocytic clearance in Parkinson's disease. Mol. Neurodegener. 14 (1), 16. https://doi.org/10.1186/s13024-019-0314-8.

Troncoso-Escudero, P., Parra, A., Nassif, M., Vidal, R.L., 2018. Outside in: unraveling the role of neuroinflammation in the progression of Parkinson's disease. Front. Neurol. 9, 860. https://doi.org/10.3389/fneur.2018.00860.

Tysnes, O.B., Storstein, A., 2017. Epidemiology of Parkinson's disease. J. Neural. Transm. 124 (8), 901–905. https://doi.org/10.1007/s00702-017-1686-y.

Walsh, S., Finn, D.P., Dowd, E., 2011. Time-course of nigrostriatal neurodegeneration and neuroinflammation in the 6-hydroxydopamine-induced axonal and terminal lesion models of Parkinson's disease in the rat. Neuroscience 175, 251–261. https://doi.org/10.1016/j.neuroscience.2010.12.005.

Wang, Q., Liu, Y., Zhou, J., 2015. Neuroinflammation in Parkinson's disease and its potential as therapeutic target. Transl. Neurodegener. 4, 19. https://doi.org/10.1186/s40035-015-0042-0.

Yanuck, S.F., 2019. Microglial phagocytosis of neurons: diminishing neuronal loss in traumatic, infectious, inflammatory, and autoimmune CNS disorders. Front. Psychiatr. 10, 712. https://doi.org/10.3389/fpsyt.2019.00712.

Zahorec, R., 2021. Neutrophil-to-lymphocyte ratio, past, present and future perspectives. Bratisl. Lek. Listy 122 (7), 474–488. https://doi.org/10.4149/BLL_2021_078.

Zeng, J., Wang, X., Pan, F., Mao, Z., 2022. The relationship between Parkinson's disease and gastrointestinal diseases. Front. Aging Neurosci. 14, 955919 https://doi.org/10.3389/fnagi.2022.955919.

Zhao, J., Zhang, W., Wu, T., Wang, H., Mao, J., Liu, J., Zhou, Z., Lin, X., Yan, H., Wang, Q., 2021. Efferocytosis in the central nervous system. Front. Cell Dev. Biol. 9, 773344 https://doi.org/10.3389/fcell.2021.773344.

Zhu, B., Yin, D., Zhao, H., Zhang, L., 2022. The immunology of Parkinson's disease. Semin. Immunopathol. 44 (5), 659–672. https://doi.org/10.1007/s00281-022-00947-3.